

Experimental Study and Numerical Simulation of Rock Fracture Caused by Rapid Decompression of Sub/Supercritical Fluid

Nobuo HIRANO, Kenta TAKAGI and Noriyoshi TSUCHIYA

Graduate School of Environmental Studies, Tohoku University

6-6-20 Aramaki-Aza Aoba, Aoba-ku, Sendai, 980-8579 JAPAN

nhirano@geo.kankyo.tohoku.ac.jp

Keywords: rapid decompression (flashing), fracturing, sub/supercritical fluid, granite

ABSTRACT

The formation of artificial cracks in rocks can be applied to the drilling of deep geothermal reservoirs. The temperature drops and thermal stress derived from rapid decompression are considered to be effective for fracture initiation in rock. In this study, we performed rapid decompression experiments of granite samples under supercritical and subcritical fluid conditions using an autoclave. Adiabatic expansion by rapid decompression of the fluid in the autoclave reduces the temperature of the granite sample. The experimental results show that the porosity of the decompressed granite sample depends greatly on the temperature drop. The strain value of the granite sample was calculated from the temperature drop of the granite and the linear thermal expansion coefficient, and it was found that there is a good relationship between the calculated strain value and the porosity change. This change in porosity indicates the growth of fractures within the granite sample. The strain distribution inside the granite sample was calculated using FEM simulation software (Dassault Systems Abaqus). As a result, the strain value was large at different mineral grain boundaries, and the distribution showed the same tendency as the fracture distribution of the decompression sample. Therefore, it is thought that it is possible to generate fractures in rock by internal thermal stress using rapid decompression with temperature drop of the fluid.

1. INTRODUCTION

As a new target of geothermal power generation, research on supercritical geothermal power generation, which is considered to have a greater potential to reduce greenhouse effect gas emissions than conventional power plants, has been advanced in recent years. According to previous researches, in Japan, it is estimated that over 400 °C supercritical water originating from mantle-derived magma exists at 3-5 km depth in a volcanic area that satisfies certain conditions (CSTI, 2016). The supercritical geothermal power generation is a method that uses higher temperature and higher pressure geothermal resources than before, and the resources may be widely distributed, so it is expected to realize large power generation per power plant. In addition, the development is expected to be independent from natural hydrothermal systems (e.g. hot springs) and to reduce the risk of induced earthquakes around the geothermal reservoir. So, it may be possible to make agreement with local residents relatively easy, with regard to issues such as coexistence with hot springs. For practical application and development of the supercritical geothermal power generation, it is necessary to develop a high temperature deep-seated geothermal reservoir and to form a fracture network with high heat extraction performance. Granitic rock which constitutes the major part of the continental crust of Japan, is subject to plastic deformation during opening and closing of fractures in the rock when the temperature is over 360 °C in a high-pressure environment at a depth of 2 km or more. Therefore, it has been considered that the permeability was drastically reduced and the formation of the geothermal reservoir would be difficult. However, Watanabe et al. (2017) suggested that such an assumption might not hold, that is, geothermal development is feasible also in the plasticity region. It was clarified that there is a condition that can maintain high permeability which would enable such development (Figure 1). This suggests that the formation of fracture networks and generation of supercritical geothermal reservoirs is possible in deep seated zones. As a well stimulation method for forming a fracture network, currently the main method is hydraulic fracturing in which cracks are generated in a rock body by injecting water under high pressure. However we propose decompression fracturing as a new fracturing method. Decompression fracturing is a new method of forming a fractured layer by thermal shock generated inside the rock by using rapid temperature drop accompanying fluid phase change due to rapid decompression of fluid at high temperature and pressure. Some of this effectiveness has been reported in Master's theses of our university (e.g. Kasahara, 2015, Aoshima, 2016).

2. EXPERIMENTAL METHOD

2.1 Experimental Apparatus

Figure 2 shows an overview and photographs of the experimental setup used in this research. As the material of the autoclave, Inconel625 is used for the main body and upper and lower flanges, and the other attached piping is made of SUS316. The reaction chamber of the autoclave has a diameter of 66 mm, a depth of 105 mm and a volume of 380 cm³. The upper limit temperature and pressure are 600 °C and 60 MPa. The autoclave is heated and controlled by an electric furnace. The pressure in the reaction chamber changes depending on the amount of the distilled water (filling rate) to be enclosed. So even under the same temperature conditions, various pressure conditions can be obtained by changing the filling rate of water. Two pipes are attached to the upper flange. One pipe is connected to a pressure gauge and can directly measure the pressure inside the reaction chamber. Furthermore, this pipe can be open to the outside through a stop valve. By opening this valve, the hot water and steam in the reaction chamber can be released from the autoclave, and rapid decompression inside the reaction chamber can be performed. The rapid decompression inside the reaction chamber occurs at the tip of the capillary tube (70 mm below from the upper flange) directly connected to the valve. The other pipe is used to insert the thermocouple into the reaction chamber. The tip of the thermocouple is at the same position as the tip of the capillary tube for decompression, and the temperature near the pressure generation point can be

measured. Changes in temperature and pressure during the decompression experiment were recorded by a data logger (Graphtec GL220).

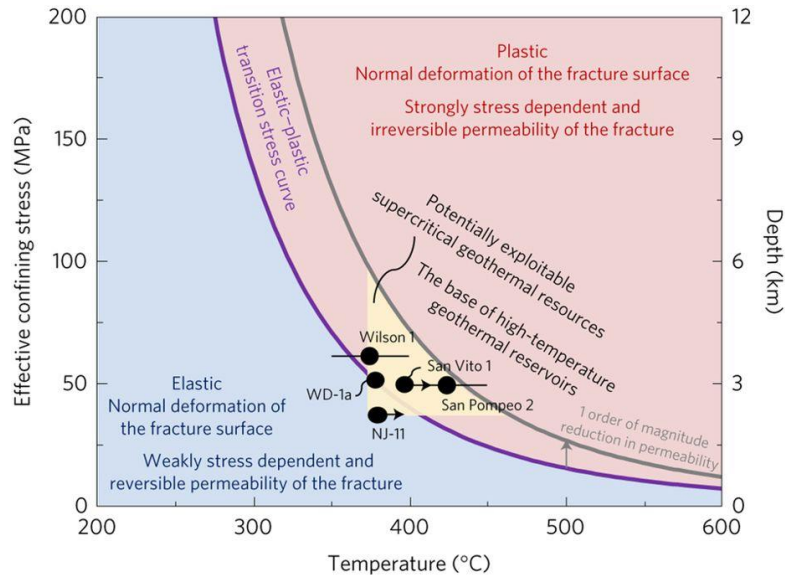


Figure 1: Temperature and effective confining stress (depth) conditions for the base of high-temperature geothermal reservoirs, and potentially exploitable supercritical geothermal resources. (Watanabe et al., 2017)

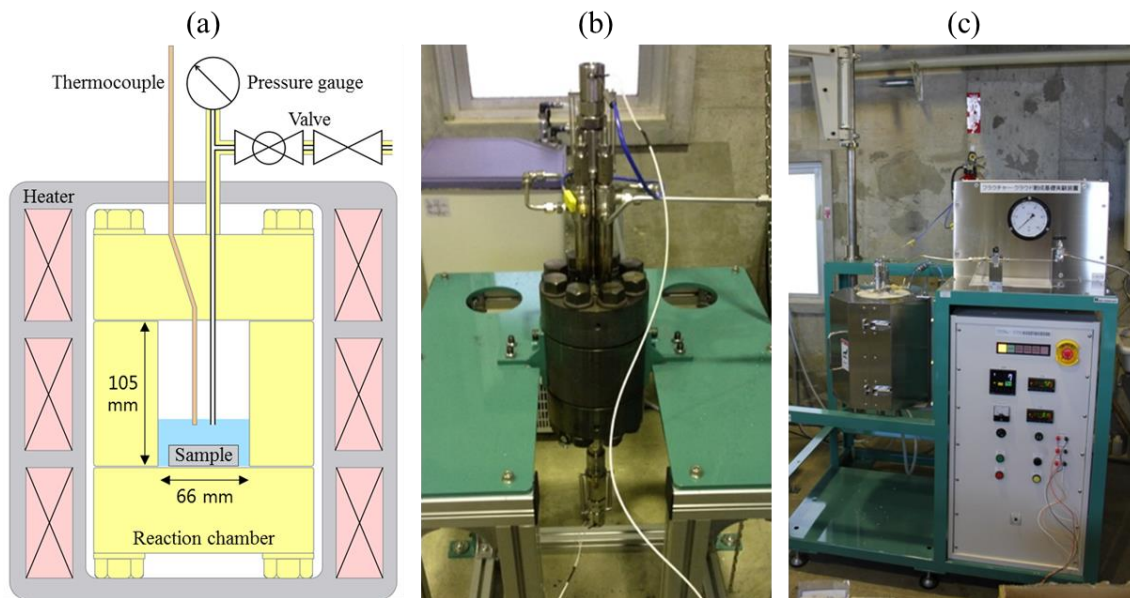


Figure 2: Schematic illustration of the experimental apparatus. (b) Photograph of the autoclave. (c) Overall view.

2.2 Experimental Samples and Procedure

The rock samples used for the rapid decompression experiments were Iidate granite from Fukushima Prefecture in Japan. Modal composition of main component minerals of this granite is 37.1% quartz, 21.8% K-feldspar, 34.0% plagioclase, 6.3% biotite and 0.6% others (Liu et al., 2003). The experimental sample of granite is shown in Figure 3. The sample is rectangular in shape, about 1.5 cm × 1.5 cm × 5 cm.

The granite sample and distilled water were enclosed in the reaction chamber, and the temperature was raised until it reaches the experimental temperature. When the temperature in the chamber reached the decompression start temperature, the condition was maintained for about 5 minutes. Thereafter, the stop valve was released and the pressure in the chamber was rapidly reduced to atmospheric pressure. By performing this operation, evaporation and adiabatic expansion of the fluid occur in the chamber, and the granite sample was cooled. In this study, the decompression experiment was conducted under three conditions: (1) in low temperature liquid phase condition at temperature 180–350 °C, (2) supercritical condition at temperature 500, 550, 600 °C, and (3) high temperature vapor phase condition at temperature 500, 550, 600 °C. Figure 4 shows the decompression start temperature and pressure of these experiments. The fracture formation of the decompressed sample after the experiment was evaluated by porosity and X-ray CT image. Porosity was measured by the difference between the water saturated weight and the dry weight of the sample. X-ray CT images were taken using a Comscantecno ScanXmate-D225.



Figure 3: Photograph of intact granite sample.

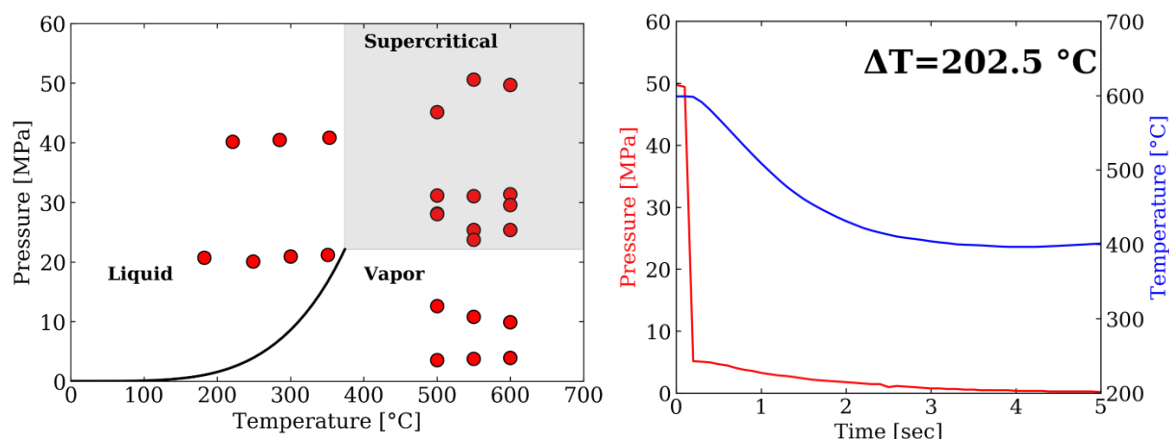


Figure 4: Conditions of rapid decompression experiments with vapor pressure curve. (left) Example of temperature and pressure changes of after decompression. (right) Example of temperature and pressure changes of after decompression.

3. EXPERIMENTAL RESULTS

Figure 5 shows the relationship between the porosity and temperature drop (ΔT). In Figure 5, the color of each plot symbol indicates the decompression start temperature, and the three plots at the left end represent the average porosity value of the samples naturally cooled from 500, 550, and 600 °C in the autoclave. The average porosity of the intact sample before the experiment was 0.5-1.0%.

In samples that were naturally cooled after being heated over 500 °C, the porosity was 1.37% (500 °C), 1.46% (550 °C), 2.54% (600 °C), which is higher than intact samples. The rapid decompression samples had a higher porosity than in the case of natural cooling, and the porosity tended to increase with the ΔT . The porosity of the sample that produced the largest ΔT after rapid decompression showed an increase of 0.44% at 500 °C, 0.76% at 550 °C, and 0.42% at 600 °C, compared to the porosity of the natural cooling sample.

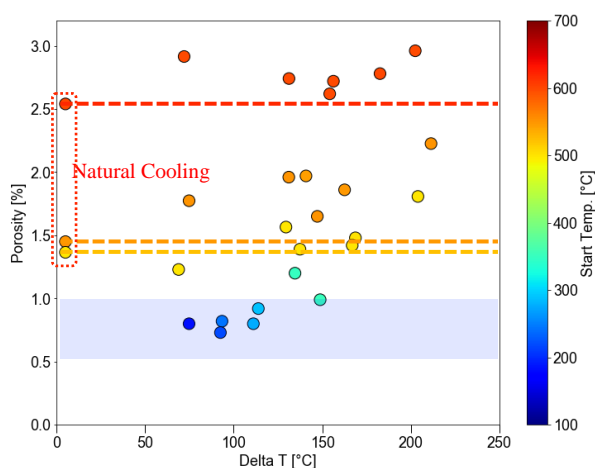


Figure 5: Porosity versus ΔT of samples after decompression. Color of each dot represents decompression temperature.

In addition, the porosity of both natural cooling and rapid decompression samples increased with decompression temperature increase. In particular, the porosity increased significantly between 550 °C and 600 °C. This is considered to be largely affected by the volume change and the strain occurrence due to the α - β phase transition at 573 °C of quartz grain. Also, previous studies show that the bulk modulus of single quartz crystals decreases significantly before and after the α - β phase transition of quartz (Ohno, 1995) and that the crack density in granite increases (Lin, 2002).

On the other hand, in the rapid decompression experiment at temperatures of 350 °C or under, the porosity of the samples that had decompression start temperature of 180 to 300 °C were 0.73 to 0.92%. These porosities are almost the same as that of the intact sample. However, when the decompression start temperature was 350 °C, the porosity showed a value of 0.99% to 1.20%, which was a slight increase from the intact granite before the experiment.

The relationship between the amount of strain change ($\Delta\epsilon$) and porosity of the decompression sample is shown in Figure 6. The $\Delta\epsilon$ of decompression samples are the strain at the decompression temperature minus the strain at the after-decompression temperature. $\Delta\epsilon$ of natural cooling samples are the strain at each maximum temperature minus the strain at the room temperature. That strain was calculated from the linear expansion coefficient of granite quoted from Heuze et al. (1983). As a result, it was found that the strain in the sample by decompression and the porosity show a good correlation. Also, at the same strain, the rapid decompression sample shows larger porosity than the natural cooling sample. The rapid decompression sample is also cooled down to room temperature, as with the naturally cooled sample. Therefore, the thermal strain generated in the sample is the same. The difference between these samples is whether the rate of thermal strain generation is fast or slow. This result indicates that the temperature drop by decompression is effective as a fracturing method for granite.

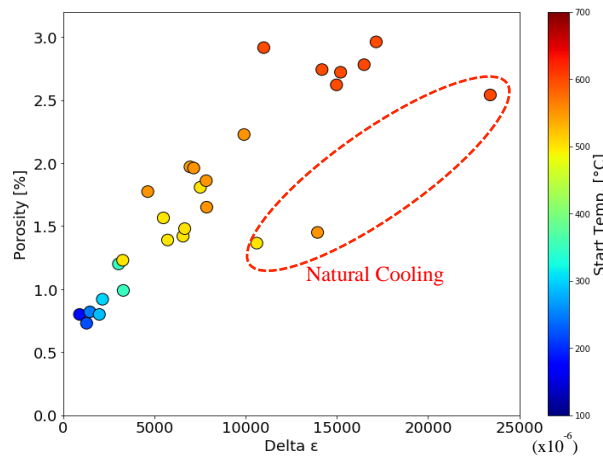


Figure 6: Porosity versus $\Delta\epsilon$ of samples after decompression. Color of each plot represents decompression temperature.

The X-ray CT images of the samples after the experiments at 500 °C, 550 °C and 600 °C are shown in Figure 7. In the decompression sample at 600 °C, several clear fractures were observed as indicated by the arrows in the figure. These fractures appear to grow along mineral grain boundaries. It is considered that this is because the grain boundary breaks as a result of the accumulation of strain at the mineral grain boundary. As the experimental temperature decreases to 550 and 500 °C, no clear fractures were observed. However, because the porosity of the sample is increasing, it is considered that microfractures are generated inside the sample.

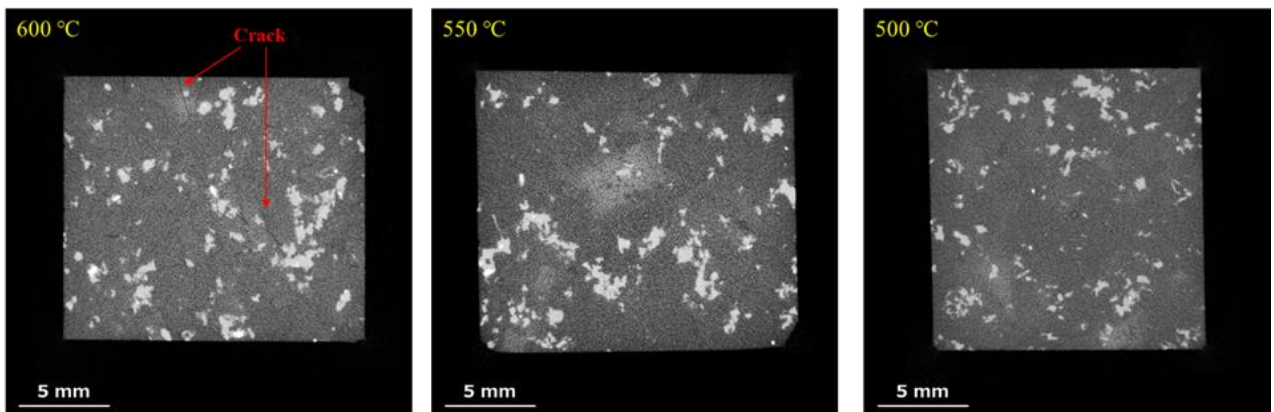


Figure 7: X-ray CT images of samples after rapid decompression experiments at 500, 550 and 600 °C.

4. FEM SIMULATION OF THERMAL STRESS DISTRIBUTION

In this study, Abaqus manufactured by Dassault Systemes was used as finite element method analysis software. Abaqus is widely used in industrial and scientific research in various fields. The solver used Abaqus/Standard, which performs finite element analysis using an implicit method, and preparation of analysis models and display of analysis results were performed on Abaqus/CAE.

The analysis model was created based on a granite sample of 5 cm outer diameter and 1 cm center borehole diameter. This model is composed of quartz, orthoclase and biotite. The physical properties of each mineral grain in the analysis model were assumed to be isotropic, and the density, Young's modulus, Poisson's ratio, thermal expansion coefficient, specific heat, and thermal conductivity were set respectively. For physical property values other than specific heat and thermal conductivity, temperature-dependent data reported by [Hacker and Abers \(2004\)](#) were used. For the specific heat, temperature-dependent data reported by [Holland and Powell \(2011\)](#) were used. As for thermal conductivity, temperature-dependent data reported by [Kanamori et al. \(1968\)](#) for quartz and by [Weidenfeller et al. \(2002\)](#) for orthoclase were used respectively. However, temperature-dependent data of thermal conductivity of biotite could not be obtained from the literature. Therefore, the value of thermal conductivity of biotite was set at 2.02 W/m·K regardless of the temperature. [Figure 8](#) shows the analysis model and analysis mesh created under these model condition. This model simulates the case of temperature drop by decompression around a borehole in granite rock. In this model, the mineral grain boundaries are fixed, and no deformation or destruction of the mineral occurs. The red line in the model is the temperature drop profile obtained from the decompression experiment. For the analysis, the initial temperature of the entire model was set to 550 °C, and the temperature drop profile obtained from the experiment was used. The analysis time step was 0.1 seconds, and 200 steps were analyzed, total 20 seconds. Regarding the flow of analysis, first, heat transfer analysis of the model was performed to determine the time variation of temperature distribution in the model. Next, the time variation of the analyzed temperature distribution was given again to the same analysis model, and the time variation of the Mises stress generated in the model was determined.

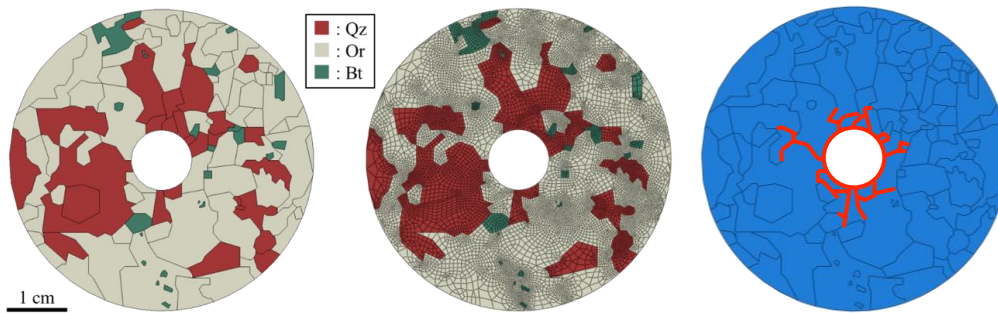


Figure 8: Analysis model (left), analysis mesh (right) and where the temperature drop profile was given (right). Qz: quartz, Or: orthoclase and Bt: biotite.

[Figure 9](#) shows the analysis results of temperature distribution and stress distribution in the analysis model at 1, 3 and 5 seconds after the start of cooling. With regard to the temperature distribution, cooling proceeds to half of the model radius in 5 seconds after the start of cooling, but cooling of the entire model has not been achieved. Moreover, as the cooling region expanded, the region in which stress was generated was also expanded, but the stress was also generated in the region where the temperature drop did not occur. This suggests that the fracture may generate even in the part that is separated from the cooling region and is not affected by the temperature drop. The generated stress was concentrated at grain boundaries between quartz and orthoclase or quartz and biotite. This is considered to be because the linear expansion coefficient of quartz is larger than the other minerals. This stress distribution means that fractures are likely to occur at mineral grain boundaries between quartz and other minerals, and it is similar to a fracture as shown in [Figure 7](#).

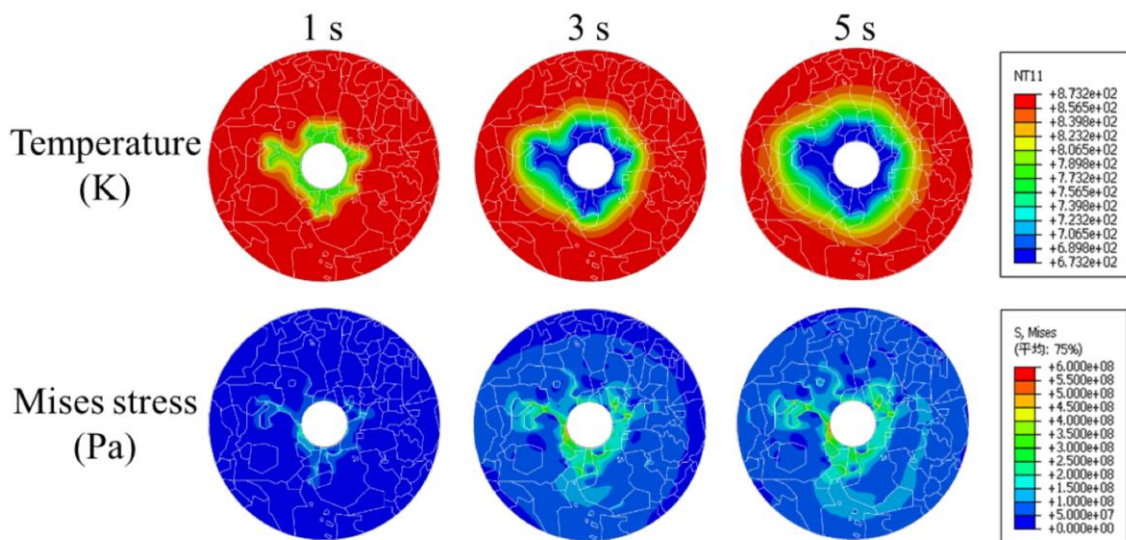


Figure 9: Analysis results for 5 seconds after decompression with Abaqus. The upper part is the temperature distribution, and the lower part is the Mises stress distribution.

5. CONCLUSIONS

In this study, fracture formation experiments were conducted on granite samples using temperature drop due to rapidly pressure reduction, under various temperature and pressure conditions. A rapid temperature drop occurred immediately after decompression in all experiments. This is because the phase change of the fluid occurs with the rapid pressure reduction. The porosity of the sample after decompression experiment showed a clear increase when the decompression start temperature was over 350 °C. In experiments at over 500 °C, the porosity of the naturally cooled sample increased. However, in the rapid decompression and temperature drop experiment, the porosity increased more than in the case of the natural cooling experiment. By calculating the stress distribution inside the rock using Abaqus FEM simulation, it was found that stress is concentrated at grain boundaries between quartz and other minerals in the case of granite. This indicates that the fracturing by temperature drop is generated from the quartz-other mineral grain boundary. From these results, it is seen that it is possible to generate fractures by thermal stress inside the rock using rapid decompression with temperature drop of fluid. This phenomenon is named as decompression fracturing. In addition, because decompression fracturing is likely to occur around quartz grains inside the rock, it is considered to be an effective application for high temperature rocks that contain quartz.

ACKNOWLEDGEMENT

This research is based on results obtained from a project "Supercritical Geothermal Power Generation Technology R & D (P18008)" subsidized by the New Energy and Industrial Technology Development Organization (NEDO).

REFERENCES

- Aoshima, N.: Experimental study of rock fracturing by phase change of fluid, *Master Thesis*, Tohoku University (2016).
- Council for Science, Technology and Innovation: National Energy and Environment Dstrategy for Technological Innovation towards 2050, *Reports*, Cabinet Office JAPAN (2016).
- Hacker, B. R., & Abers, G. A.: Subduction Factory 3: An Excel worksheet and macro for calculating the densities, seismic wave speeds, and H₂O contents of minerals and rocks at pressure and temperature, *Geochemistry, Geophysics, Geosystems*, **5**(1), (2004).
- Heuze, F. E.: High-temperature Mechanical, Physical and Thermal Properties of Granitic Rocks- A Review, *Int.J.RockMech. Min. Sci. & Geomech. Abstr.*, **20**(1), (1983), 3-10.
- Holland, T. J. B., & Powell, R.: An improved and extended internally consistent thermodynamic dataset for phases of petrological interest, involving a new equation of state for solids. *Journal of Metamorphic Geology*, **29**(3), 333-383.
- Kanamori, H., Fujii, N., & Mizutani, H. (1968). Thermal diffusivity measurement of rock - forming minerals from 300 ° to 1100 °K, *Journal of geophysical research*, **73**(2), (2011), 595-605.
- Kasahara, N.: Experimental study of generation of rock fracture by phase change of fluid under sub-supercritical conditions, *Master Thesis*, Tohoku University (2015).
- Lin, W.: Permanent strain of thermal expansion and thermally induced microcracking in Inada granite, *Journal of Geophysical Research: Solid Earth*, **107**(B10), (2002).
- Liu, L., Suto, Y., Bignall, G., Yamasaki, N., & Hashida, T.: CO₂ injection to granite and sandstone in experimental rock/hot water systems, *Energy Conversion and Management*, **44**(9), (2003), 1399-1410
- Ohno, I.: Temperature variation of elastic properties of ALPHA-quartz up to the ALPHA- BETA transition, *J. Phys. Earth*, **43**, (1995), 157-169.
- Watanabe, N., Numakura, T., Sakaguchi, K., Saishu, H., Okamoto, A., Ingebritsen, S. E., & Tsuchiya, N.: Potentially exploitable supercritical geothermal resources in the ductile crust, *Nature Geoscience*, **10**(2), (2017), ngeo2879.
- Weidenfeller, B., Höfer, M., & Schilling, F.: Thermal and electrical properties of magnetite filled polymers, *Composites Part A: Applied Science and Manufacturing*, **33**(8), (2002), 1041-1053.